

Review

The Main Controlling Factors on the Evolution of the Cambrian Carbonate Platform in the Tarim Basin and Its Implications for the Distribution of Ultra-Deep Dolomite Reservoirs

Kehui Zhang ^{1,2}, Xuelian YOU ^{1,2,*}, Yifen Wu ^{1,2}, Yijing Zhao ^{1,2} and Jia Wang ^{1,2}¹ School of Ocean Sciences, China University of Geosciences, Beijing 100083, China² Marine and Polar Research Center, China University of Geosciences, Beijing 100083, China

* Correspondence: youxuelian@cugb.edu.cn

Abstract: Cambrian age strata are the critical development and research stratum series of oil and gas reserves in the Tarim Basin, which contains rich oil and gas resources. The restoration of the Cambrian carbonate platform conversion and the main control factors of development has significant implication for the distribution of ultra-deep dolomite reservoirs. Based on a large number of drilling and outcrop profile data, the micro geomorphic characteristics of carbonate platforms in different periods of the Cambrian period are reconstructed in the western Tarim area, and the basin filling and structure, paleoclimate, sea level change, and seawater redox conditions are combined to analyze the main controlling factors of platform development in different periods and establish the platform evolution model. The characteristics and evolution of the Cambrian Tarim prototype basin are mainly controlled by the break-up of the Rodinia supercontinent, and its tectonic sedimentary pattern has evolved from the north–south differentiation pattern at the end of the Ediacaran to the east-west differentiation pattern of the Cambrian. The sedimentary framework of the Terreneuvian was mainly controlled by the development of paleo-uplift caused by structure and the change of seawater properties caused by the sea level variation. In the Series2 carbonate platform with extensive development, the internal differentiation is controlled by the new paleogeographic pattern of “three uplifts and two depressions”, and reef beach facies belt and platform edge begin to develop due to the lowering of sea level. Under the combined action of rapid accumulation of carbonate rocks, gradual stabilization of global sea level, and the change of ancient climate from warm and humid to hot and dry, the platform environment in the west of the Tarim Basin changed from a restricted platform environment to an evaporation platform environment, and the evaporation lagoon area in Bachu was significantly expanded in the Miaolingian. During the Furongian, the basin ended the evaporation lagoon sedimentary environment mainly due to the rise of sea level and developed a restricted platform environment again.

Keywords: Cambrian; Tarim Basin; carbonate rock; paleogeomorphology; geochemistry; dolomite

Citation: Zhang, K.; YOU, X.; Wu, Y.; Zhao, Y.; Wang, J. The Main Controlling Factors on the Evolution of the Cambrian Carbonate Platform in the Tarim Basin and Its Implications for the Distribution of Ultra-Deep Dolomite Reservoirs. *Minerals* **2023**, *13*, 245. <https://doi.org/10.3390/min13020245>

Academic Editors: Jenna Poonoosamy and Felix Brandt

Received: 11 January 2023

Revised: 1 February 2023

Accepted: 6 February 2023

Published: 9 February 2023



Copyright: © 2023 by the authors. Licensee MDPI, Basel, Switzerland. This article is an open access article distributed under the terms and conditions of the Creative Commons Attribution (CC BY) license (<https://creativecommons.org/licenses/by/4.0/>).

1. Introduction

The Lower Paleozoic carbonate rock series in the Tarim Basin still contains rich oil and gas resources [1,2]. In the oil source rock correlation study, the lower Paleozoic cratonic interval in the basin has two main sources: the Middle–Upper Ordovician and the Cambrian Lower Ordovician [3–10]. Cambrian sub-salt dolomite has become an important strategic replacement area for deep to ultra-deep oil and gas exploration in the Tarim Basin. Restoring the Cambrian carbonate sedimentary environment is an important basis for studying the filling evolutionary history of the Tarim Basin and predicting the Cambrian favorable reservoir facies (areas). Therefore, the analysis of the main controlling factors of the development of the Cambrian carbonate platform in the Tarim Basin is not only conducive to revealing the coupling relationship between the evolution of the Cambrian

Tarim Basin and the marine environment, but also conducive to deepening Cambrian oil and gas exploration, which has important theoretical and exploration significance.

Lower Paleozoic carbonate sequences in the Tarim Basin are mainly deposited on shallow marine carbonate platforms, and dolomitization is widespread [11,12]. Among them, evidence of microbial-mediated primary dolomite in the ancient Sabkha environment was found in the Cambrian thick dolomite stratum [13–17]. Jia et al. [18–20] carried out research on geotectonic analysis and sequence lithofacies paleogeography for Cambrian sub-salt dolomite structure lithofacies paleogeography in the Tarim Basin. It is proposed that the Cambrian Tarim plate has the east–west differentiation pattern of “two platforms sandwiched with one basin”, the terrain difference between the south and the north, and the formation sequence of gentle slope strong border. Wu et al. [21–24] explored the internal geological structure of the western Tarim Basin and its control of the sedimentary differentiation of the overlying carbonate platform. They subsequently proposed the development of the Awati–Manjiaer rift in the Precambrian and the “Three-rise and two-depression” pattern developed in the Early Cambrian. Wei et al. [25–28] reconstructed the prototype basin of the Cambrian in Tarim and discussed the Cambrian lithofacies paleogeography. It is believed that the siliceous rock and mudstone strata in the Kaping area belong to basin slope facies and the carbonate rock strata belong to platform margin sedimentary facies. Zheng et al. combined geochemical techniques to restore the ancient environment, especially to guide the temperature, sea level rise and fall, and redox conditions [29–32]. With the deepening of exploration, the emergence of new materials and data provides a new basis for further research on the evolution of the carbonate platform in the west of Tarim, but research that can comprehensively use big data to analyze and explore the main controlling factors of the evolution of the carbonate platform is insufficient. This paper mainly integrates the published data to restore the paleogeomorphology of the carbonate platform in the west of Tarim and analyzes the main controlling factors of its development, providing a new perspective for the distribution of ultra-deep dolomite reservoirs.

2. Geological Setting

The Tarim Craton in northwestern China covers an area of $56 \times 10^4 \text{ km}^2$ and is one of the three Chinese Craton (the other two are the North China Craton and the Yangtze Craton). The basin is tectonically surrounded by the Tianshan orogenic belt in the north, the West Kunlun orogenic belt in the southwest, and the Altun orogenic belt in the southeast [33,34], and the tectonic pattern of the basin is “four uplifts and five depressions”. The four uplifts are the Tabei Uplift, the Bachu Uplift, the Tazhong Uplift, and the Tadong Uplift, and the five depressions are The Kuqa Depression, the North Depression, the Southwest Depression, the Southeast Depression, and the Tanggu Depression (Figure 1a).

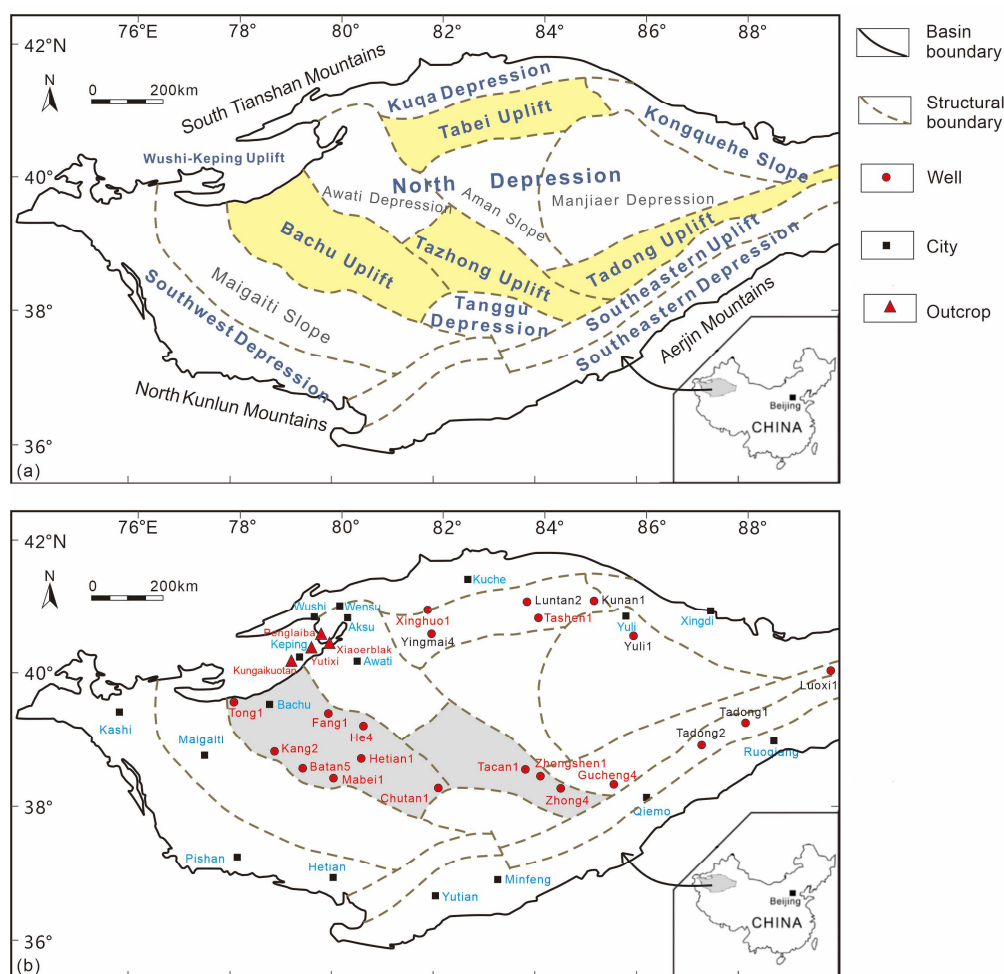


Figure 1. (a) Structural unit division of the Tarim Basin [35]. (b) Distribution of major cities, outcrops, and well drilling locations in the Tarim Basin, where the location of the study area is marked in gray and the outcrop and drilling wells with names in red font are the sample sites for this study.

The Tarim Block is a small-scale craton block drifting in the Proto-Tethys Ocean, which probably belonged to the same Rodinia supercontinent as the Australian and the Yangtze plate in the Neoproterozoic, probably at the northwestern margin of the Gondwana paleocontinent. The Tarim Basin is a large stacked basin of continuous sedimentation with complex tectonic evolution, forming different types of primitive basins at various stages [33,36]. The basin basement was formed by differential metamorphism of the Pre-Ediacaran terrestrial crust. The overlying rocks are a multi-stage superimposed sedimentary cover; the Ediacaran–Paleogene marine sedimentary sequence is overlain by Mesozoic–Cenozoic foreland and intra-land sedimentary sequences. The basin has undergone multiple stages of structural evolution. Two tectonic events occurred during the early stages of the Caledonian tectonic events. The first act, known as the Keping tectonic events, occurred at the end of the Aurignacian and resulted in a regional unconformity (T90) between the igneous rocks of the Upper Ediacaran and the Lower Cambrian. The second act began at the end of the Cambrian. It continued into the Early Ordovician, forming a regional unconformity (T80) between the Lower Qiulitage Formation of the Furongian and the Penglaiba Formation of the Lower Ordovician [34] (Figure 2). This study focuses on the Keping area and the central uplift zone at the northwest margin of the Tarim Basin (Figure 1b). This study focuses on the Keping area and the central uplift zone at the northwest margin of the Tarim Basin. Geochemical data from four sections and lithological analysis from 14 drilling wells were referenced and combined to explore the evolution of the carbonate platform.

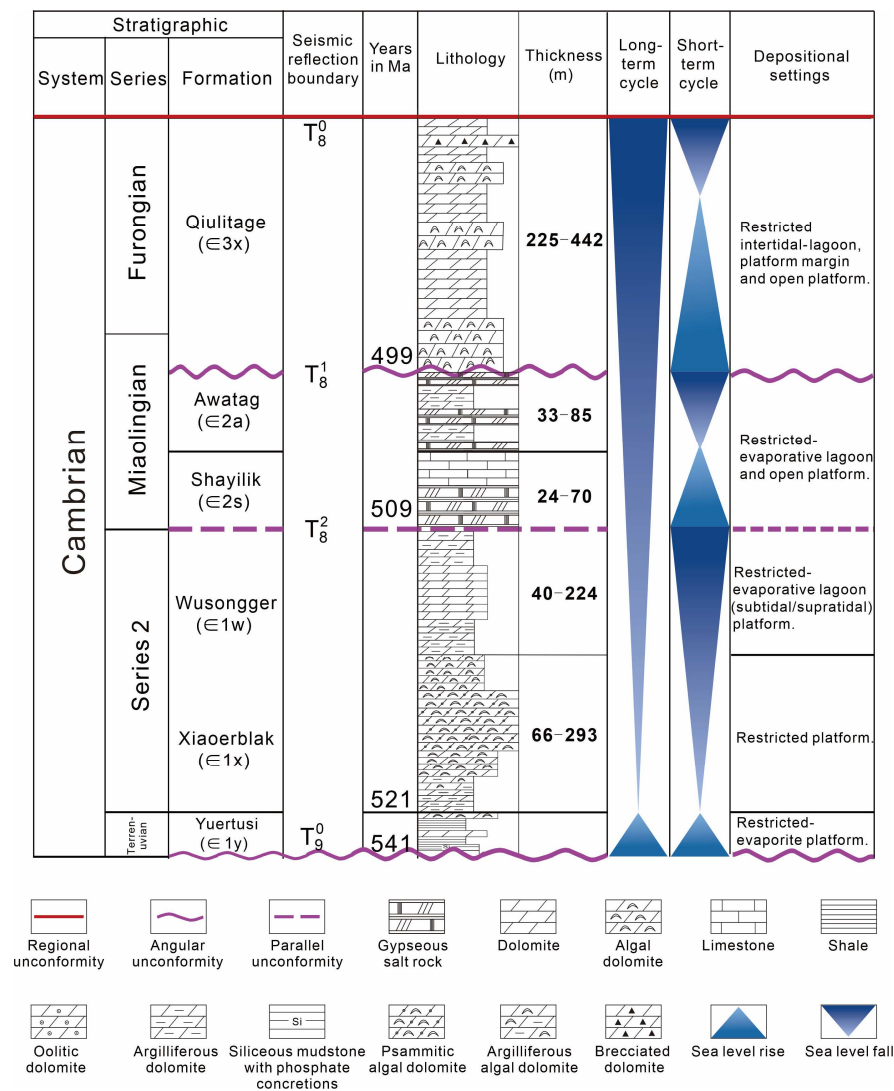


Figure 2. Evolution of Cambrian strata, unconformity, sedimentary environment, and main periods in the central and western Tarim Basin [37,38].

3. Characteristics of Cambrian Lithofacies and Paleogeography

In the Cambrian system, the western Tarim Basin can be divided into the following four sub-sequences: Terreneuvian, mainly developed the Yuertus Formation; Series2, including the Xiaerblak Formation and Wusongger Formation; Miaolingian, including the Shayilik Formation and Awatag Formation; and Furongian includes the Lower Qiulitage Subgroup (Figure 2) [9,34,37,39,40].

3.1. Terreneuvian

From Terreneuvian to Series2, the Tarim Craton exhibited a characteristic of a west-east differentiation structure, including the Taxi Platform, Luoxi Platform, and a starved basin named Tadong Basin [11,41,42]. In early Terreneuvian, due to the intensification of the break-up along the margin of Tarim, a large amount of seawater entered the Tarim Craton, and the carbonate sediments of Ediacaran were submerged, making the rapid transgression at early sedimentary of the Yuertus Formation [35]. There was an ancient continent that was not submerged by seawater in the Bachu–Tazhong area. The records of ⁸⁷Sr/⁸⁶Sr and δ¹³C and seismic profiles indicate the existence of carbonates paleo-uplift [43]. The trend of the paleo-uplift is NW to SE. In the late Ediacaran, the area of the paleo-uplift was large and mainly concentrated in the Bachu–Tazhong area. With the rise of the sea

level, the area of the paleo-uplift gradually decreased while the area of sedimentary was increased. The top of the Yuertus Formation of exploratory well Fang1 is pure dolomite and the overlying Xiaerblak Formation deposited continuously after it, indicating that the ancient continent in the Bachu area has been submerged by seawater due to the rise of sea level in the late stage of the Yuertus Formation sedimentation. Thus, there was no provenance area in the basin. The vast area in the west of Tarim entered the stage of carbonate platform construction [26].

In the Keping area, the Yuertus Formation is distributed widely and stably. At the bottom of the Yuertus Formation, a thin layer of siliceous rock is developed and then transits into interbed of thin layers of siliceous rock and black-gray shale rich in organic matter. In the middle, black shale and medium-thick layers of dolomite are developed and then they transit into the interbed of black-grey shale and limestone. A thick layer of dolomite is developed at the top. The underlying Upper Ediacaran Qigebulak Formation is in parallel disconformable contact with the Yuertus Formation [44,45]. During this time, shore-to-deep-water shelf facies were developed, which belonged to gentle slope platform deposition, and the Keping area evolved from the middle outside gentle slope into the middle gentle slope mound-shoal [30,46] (Figure 3). With an average thickness of about 20 m, the sedimentary layer of the Yuertus Formation is quite thin and is slightly thickened from southwest to northeast. The sedimentary center was located in the Manjiar Depression, and the sedimentation was overcompensated. It reflects that the water depth gradually becomes shallow and it is formed in an anoxic to hypoxic environment (Figure 3).

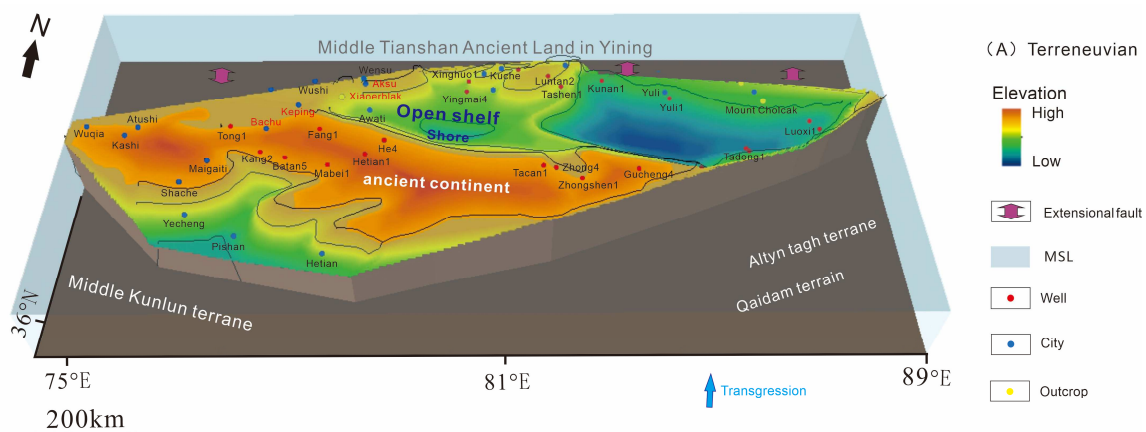


Figure 3. Sedimentary paleogeomorphic characteristics of Cambrian terreneuvian in the Tarim Basin [26,27,29–31,35,38,43,44,47–51].

3.2. Series2

The sedimentary stage of the Xiaerblak Formation was a transitional period from a gentle slope platform to a restricted platform, and the internal differentiation was controlled by the new paleogeographic pattern of “three paleo-uplifts and two depressions”. The three paleo-uplifts were the Wuqia paleo-uplift, the Tanan paleo-uplift, and the Keping-Wensu paleo-uplift, and the two depressions were the Southwest Depression and the North Depression (Figure 4). The Keping area mainly developed medium gentle slope mound-shoal deposits, showing a structure of “small mound but big shoal”. With gentle and low landforms, the Bachu area, located between the Tanan Uplift and Wuqia Uplift, mainly developed middle gentle slope mound-shoal and inner gentle slope depression deposits. The three intra-platform uplifts controlled the distribution and scale of the gentle slope mound-shoal belt in the Xiaerblak Formation [27].

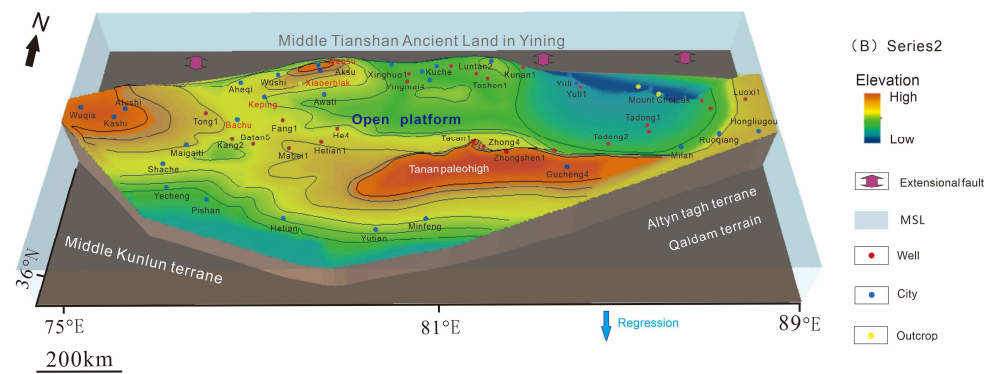


Figure 4. Sedimentary paleogeomorphic characteristics of Cambrian Series2 in the Tarim Basin.

During the period of Wusongger Formation sedimentation, the intra-platform uplifts of Tanan, Wuqia, and Keping–Wensu existed and controlled the intra-platform differentiation. However, Lunnan underwater low uplift, and medium-high energy facies were developed as the result of the continuous decline of sea level and the NE trend ancient ocean current. According to the Keping outcrop, Ketan 1, Lun 1, Lun 3, Zhonghan 1, and other drilling wells and seismic data, it was found that the platform margin in the Wusongger Formation is a weak rimmed carbonate platform during its sedimentation, marking the formal formation of the “East Basin and West Platform” pattern in the Tarim Basin. In the Keping area, the Wusongger Formation is mainly composed of an interbed of thin to extremely thin layer dolomitic mudstone and thin layer dolomite, or an interbed of thin layer argilliferous dolomite and thin layer dolomite, with the majority of tidal flat deposits. Dolomite, argilliferous dolomite, and gypsum salt rock are mainly developed in the Bachu area, which is a restricted platform of lagoon facies deposits [32]. The argilliferous content is significantly higher than that of the Xiaoerblak Formation, indicating that the water exchange in the northwest edge of the basin was more impeded during this period and the sedimentary environment was in transition from a restricted platform to an evaporation platform (Figure 4).

3.3. Miaolingian

There was a tectonic-sedimentary pattern of “one basin sandwiched between two platforms” during Miaolingian in the Tarim Basin. The western part is the large Taxi Platform, and the eastern edge of the platform progradates continuously and thus migrated to the Tadong Uplift, with obvious development of paleo-uplift (Figure 5) [11,35,47]. The eastern part is the Luoxi Platform and the middle part is the Tadong deep-water basin, which is transited by a sedimentary slope.

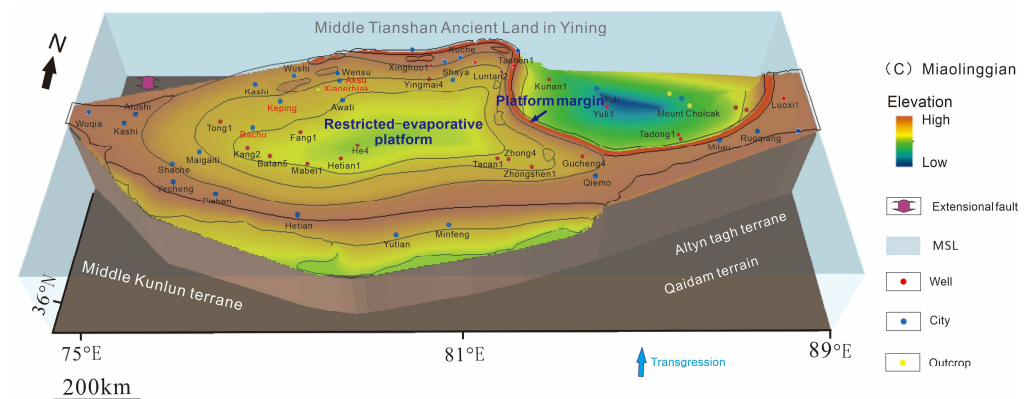


Figure 5. Sedimentary paleogeomorphic characteristics of Cambrian Miaolingian in the Tarim Basin.

The lithology of the Shayilik Formation in the Keping area is dominated by argilliferous dolomite, and the upper is karst brecciated dolomite, which indicates that the late sedimentary period of the Shayilik Formation is characterized by penecontemporaneous exposed karstification. The lithology of the Awatag Formation is yellowish-brown and grayish-red calcareous mudstone and marl, and a low-energy fragmental shoal is locally developed. The integral lithofacies show a characteristic of evaporation lagoon deposition under dry and hot climates.

Well drillings in the Bachu and Tabei areas revealed that there is mainly gypsum salt rock and gypsum mudstone, whose distribution range was significantly expanded than in the early Cambrian, indicating that the sedimentary environment in the Bachu area is more restricted. The seismic profile along the Lunnan–Gucheng platform margin shows that there is a slight thickening of the Miaolingian series in the transition zone from the platform to the slope, indicating that the original gentle slope gradient of the carbonate rock gradually increases under the gradual aggradation of the Terreneuvian–Miaolingian carbonate platform [26]. The construction of carbonate platforms has been pushed to a climax, and the range of evaporation platform facies has been continuously expanded [44]. The Shayilik Formation in the Bachu Uplift zone mainly develops restricted platform subfacies and lagoon facies. Comparing the lithofacies paleogeography of the Shayilik Formation and the Awatag Formation, it is found that the Miaolingian gypsum salt lake showed an expanding trend, with an area increased by about 1/3 (Figure 5).

3.4. Furongian

The lower Qiulitage subgroup shows a transition from microbial limestone to oolitic limestone, and most of them have experienced dolomitized [48]. The overlying Penglaiba Formation is composed of thick dolomite, intercalated limestone, or grainstone [52,53]. The drilling of Well Tashen 1 meets the upper Cambrian series platform margin facies belt, where granular dolomite and algal lamina dolomite are generally developed. Multi-stage mound-shoal bodies developed in the edge of the platform progradated more obviously toward the basin and the slope in front of the platform became larger, indicating that the platform evolved from a carbonate gentle slope to a weak-rimmed platform, and the platform edge belt became steeper and narrower (Figure 6).

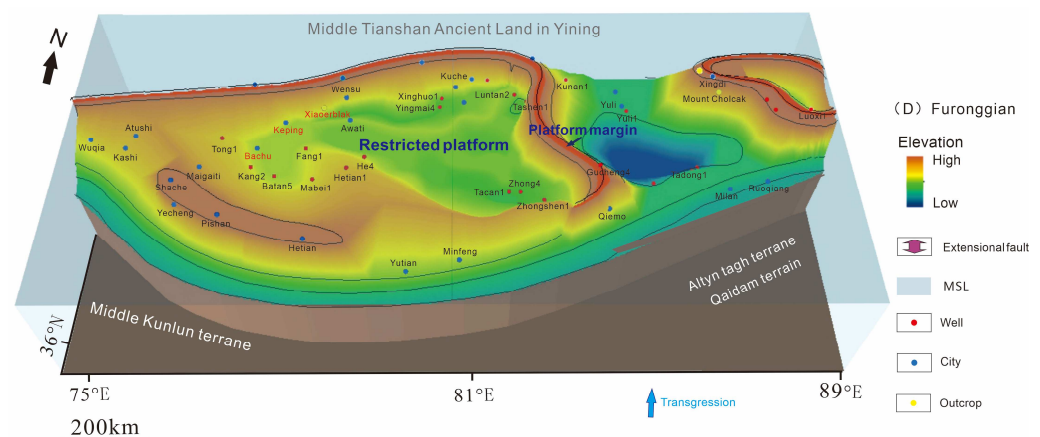


Figure 6. Sedimentary paleogeomorphic characteristics of Cambrian Furongian in the Tarim Basin.

4. Main Controlling Factors of Carbonate Platform Sedimentation

4.1. Tectonism

From the Cambrian to the Ordovician, the Tarim Basin has undergone several tectonic evolutions, from continental disintegration during lithospheric extension to craton subsidence and development of the surrounding foreland basins. The tectonic development went through two distinct phases as follows.

- 1) Regional extension from the Late Neoproterozoic to the Middle Early Cambrian, forming rift valleys, rifting, passive continental slopes, and carbonate platforms.

The Tarim–Qaidam Block, as a nearly north–south trending elongated isolated block, is located at low latitudes near the equator. The present-day orientation of the Tarim Basin is the result of an approximately 90° clockwise rotation relative to its Early Paleozoic orientation, separating the Paleo-Asian Ocean from the Proto-Tethys Ocean.

Supercontinental rifting at the end of the Neoproterozoic, with the Tarim–Qaidam Block in an extensional tectonic setting [19,54,55] flanked by passive margin environments [35,56], assembled into a series of micro-blocks on the eastern side of the Tarim–Qaidam Block (Figure 7) [57,58]. The block includes the Tarim Basin stability zone and the multi-stage marginal activity zone, surrounded by boundaries that extend to the Altun Fault Zone in the southeast, the Kansuwa Fault Zone in the southwest, and the South Tianshan North Boundary Fault Zone in the north. From the end of the Neoproterozoic to the end of the Ordovician, the Tarim–Qaidam Block was in a stretching tectonic context and behaved as a floating isolated terrace surrounded by oceans [59–62]. From the end of the Neoproterozoic to the Cambrian, the platform underwent a faulting stage, a depressional stage, and a carbonate platform stage.

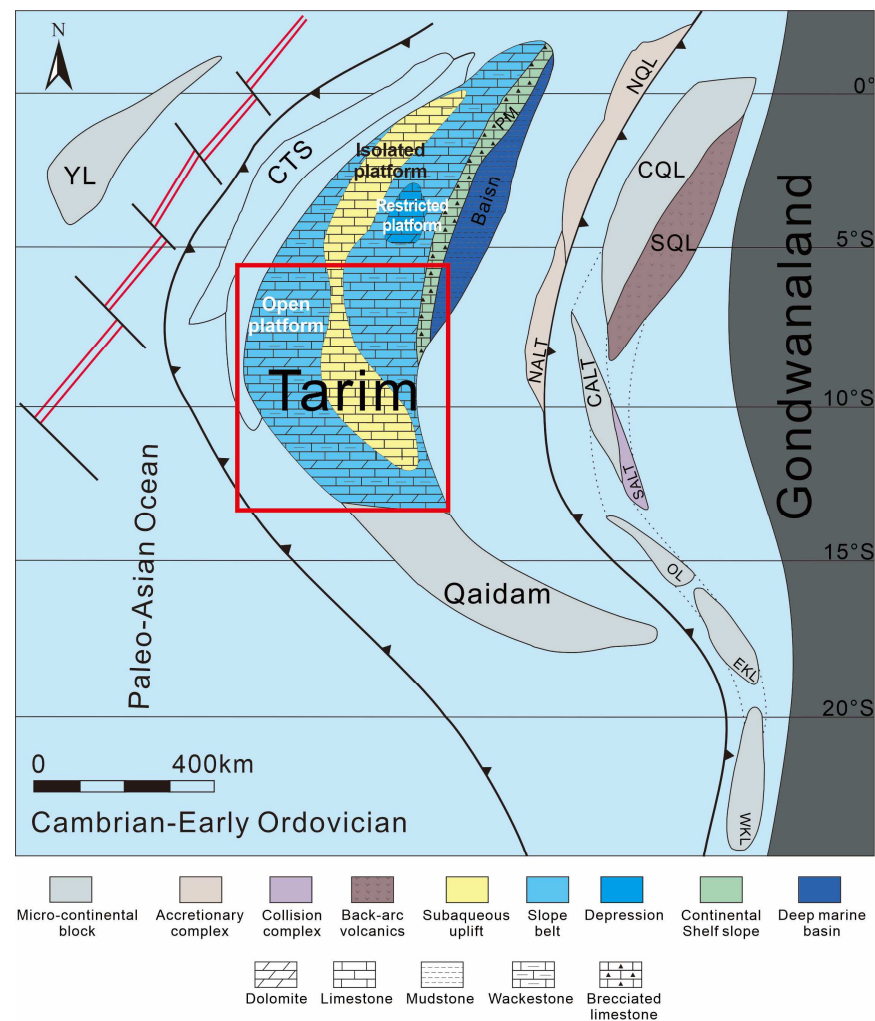


Figure 7. Tectonic and paleogeographic evolution of Tarim and its abbreviations of micro-continental blocks: NQL = North Qilian; CQL = Central Qilian; SQL = South Qilian; NALT = North Altyn; CALT = Central Altyn; SALT = South Altyn; WKL = West Kunlun; EKL = East Kunlun; OL = Oulongbuluke; CTS = Central Tianshan [56].

In the Early Cambrian, the extension of the Proto-Tethys Ocean was accompanied by subduction and collision, resulting in a nearly linear subduction system along the western flank of the microcontinent group [58]. The overall topography of the Tarim block has a high western and low eastern depositional pattern. The carbonate platform developed in the middle and west of Tarim Block and the continental rift developed around it, which formed the Manjiaer Depression in the east of Tarim Block, and slope facies and deep-water basin facies are developed between the platforms [20,61,63]. Early studies of deep geological structures found a positive magnetic anomaly belt in the Tarim Basin [64], suggesting the existence of paleo-uplift in this area. The continuous dip subduction of the Proto-Tethys Ocean plate leads to the initial bending of the Proto-Tethys subduction zone [56–58,65–68], forming an internal long underwater paleo-uplift. The isolated platform facies developed in paleo-uplift represents the form of late erosion uplift. Previous studies have shown that the uplift belt was formed during the early Cambrian to Ordovician period and mainly consisted of underwater low uplift, including the Tabei paleo-uplift and the southwestern Tarim paleo-uplift [11,69]. The palaeogeomorphology analysis shows that the Tazhong paleo-uplift is a low uplift under the background of Ediacaran to Early and Middle Cambrian fragmentation [55]. Around the underwater low uplift, open-platform carbonate dominated the Tarim Basin deposits.

- 2) A regional extension to slight extrusion from Late Cambrian to Early Ordovician, accompanied by the development of carbonate terraces and slopes of the craton.

The bending and rotation of the Tarim–Qaidam Block led to the formation of a deep-sea basin parallel to the subduction zone on the eastern margin of the plate, which gradually moved into the Tarim Basin, causing rotation, bending, and migration of paleo-uplift. Accordingly, the Tarim Basin landscape has changed, leading to differences in the sedimentary environment. The cratonic depressions in western Tarim are rapidly subsiding, while carbonate terraces, open terraces, and restricted terraces are widely developed in the basin [38,47]. The development of the Tabei paleo-uplift was accompanied by the adjacent Manjiaer paleo-uplift rift. To the northeast, the water deepens [58,69]. Between the platform and the deep-sea basin, there are continental slope break zones and carbonate clastic flow and calcite flow deposits [38]. Regionally, the Tarim Basin early Cambrian Ordovician is in a stable depositional period [56,58].

4.2. Paleoseawater Temperature

Water temperature is an important factor to control the stable oxygen isotope of carbonate, so the $\delta^{18}\text{O}$ value can be used as a reliable indicator to determine paleoseawater temperature. Quantitative analysis of palaeotemperature using $\delta^{18}\text{O}$ is often biased for Palaeozoic samples, which can be influenced by diagenesis, organic matter in sediments, and geological action, so the measured $\delta^{18}\text{O}$ needs to be evaluated and filtered. Based on the geochemical data of Cambrian dolomites measured in the Keping area, the data were filtered by correlating their carbon and oxygen isotope data with Mn/Sr ratios. Finally, it can be concluded that $\delta^{18}\text{O}$ has not been influenced by diagenesis and that the $\delta^{18}\text{O}$ in these data preserves the character of seawater [30,43,70]. The average temperature of the Yuertus Formation is 21.7 °C, which shows that the seawater in the Tarim area was in warm climate background in the early Cambrian. The Sr/Cu ratio in the early stage of the Yuertus Formation is greater than 5.0, and then it decreases to smaller than 5.0, which indicates that it is a humid–hot palaeoclimate environment [32], which is favorable to the development of living things.

The water temperature range of the Xiaerblak Formation measured by $\delta^{18}\text{O}$ is 17.8–25.0 °C, the average value is 22.1 °C, and the average sea water temperature of the Wusongger Formation is 23.6 °C, indicating that it is in the background of warm climate. The Sr/Cu ratio of the Xiaerblak Formation was higher than 5.0, the Sr/Cu ratio increased first and then decreased, and the Na and K contents increased greatly in the late stage; it shows that this period was a dry–hot climate background and the degree of dry–hot increased rapidly in the early sedimentary period. The Sr/Cu ratio of the Wusongger

Formation is lower than that of the Xiaoerblak Formation, and the total Sr/Cu ratio is greater than 5.0, showing a slow decreasing trend, which indicates that the degree of dry heat decreases slowly from the later period of the Xiaoerbulak formation to the later period of the Wusongger Formation [29,30,32].

The Sr/Cu ratio of the Shayilik Formation first increased and then decreased, with a maximum value of 196.77 and a minimum value of 15.78. The Sr/Cu ratio of the Awatage Formation first decreased to 15.59 and then increased to 115.55. The trend of Rb/Sr was basically consistent with that of Sr/Cu. It is further verified that the degree of dry heat of the Shayilik Formation was enhanced and exceeded that of the Xiaoerblak period, and that the degree of dry heat of the Awatag period was weaker than that of the Shayilik Formation [32]. The average temperature of sea water in the Shayilik Formation and Awatag Formation is 21.5 °C and 21.3 °C, respectively, measured and calculated by $\delta^{18}\text{O}$.

4.3. Relative Sea Level Change

The worldwide carbon isotope shows that the carbon isotope shows a large negative mobility in Terrenevian. Strong negative carbon isotope migration indicates the extinction of the Ediacaran fauna in the first system and the rise of sea level in the early Cambrian [71,72]. The sedimentary thin shale and siliceous rock interlayers of the Yuertus Formation gradually transited upward into clastic grainstone, and the characteristics of its grain reverse sequence reflected the upward shallowing environment and the reduction in terrigenous clastic content [44]. Based on the analysis of Mn/Ti, Mn/Fe, and Rb/K value characteristics of the Kungaikuotan section and the Xiaoerblak section in northwest Tarim, it is believed that the Yuertus Formation was a deep-water deposit in the early stage, the sea level continued to rise, and slowly decreased in the late stage, and the water depth gradually became shallow. The change of seawater salinity is affected by the rise and fall of sea level first, which is reflected in the continuous increase in Sr/Ba value and low initial salinity, which is relatively conducive to the development of organic matter, dark mudstone and high organic matter content. In the middle stage, the salinity is relatively high, and the dolomitic mudstone is deposited. At the same time, biology is not prosperous in the lower part and mudstone is light in color. At the end of the period, the salinity was the highest and the sedimentary dolomite was deposited [49].

The trace elements in the Xiaoerblak section show low Cr, Mn, Ni, Cu, Zn, and Ba values, and high Sr, Na, Fe, and Al contents, indicating that the Xiaoerblak Formation sediments are generally offshore, shallow in water depth, and rare earth elements with low ΣREE and no abnormality of Ce also indicate shallow water sedimentary environments. Lithologically, in the early stage of the deposition of the Xiaoerblak Formation, it is subtidal low-energy gray thin to middle silty fine crystal dolomite mixed with dark gray thin silicified argillaceous fine crystal dolomite. The developed outer gentle slope dolomite is darker than the upper part of the Yuertus Formation, and its mud content is increased. After the second Cambrian transgression, the water body is relatively deep. Under the wave base, it is occasionally affected by storms. In the late stage, it was the subtidal high-energy facies bright crystal gravels and sandy dolostones. At this time, the sea level was lowered, and it was the intertidal zone with a shallower sea level. Microbilites developed in a sheet shape, forming a layered coarse-grained layered agglomerate of interbedded deposition of agglomerate and muddy crystal/granular muddy dolostone. The alternating appearance of agglomerates of different sizes also reflected the high-frequency fluctuations of the seawater and was the representative of beach facies deposition at the edge of the northwest carbonate platform, It also shows the sedimentary characteristics of progradation from the platform to the basin [29,30,50]. The Xiaoerblak section is located in the tidal flat facies environment where the restricted lagoon is close to the land. The appropriate water depth provides favorable conditions for the growth and development of microorganisms. The restricted environment increases the alkalinity of seawater and the Ca and Mg ion saturation required for carbonate rock deposition. Therefore, the limited tidal flat sedimentary environment of the Xiaoerblak section in the Series2 provides favorable conditions for the development of

microbial carbonate rocks, which makes microbial rocks develop in large quantities [73]. It indicates the upward shallowing outer gentle slope microbial layer middle gentle slope microbial hill inner gentle slope microbial hill beach tidal flat sedimentary sequence [29,30]. It is noted that many layers contain argillaceous/argilliferous dolomite. Recent studies present an abiotic mechanism with high dissolved silica catalyzed dolomite precipitation, especially during early Earth history when dissolved silica concentrations were higher and subject to intense continental weathering [74,75]. The concentration of silica should also increase with increasing Mg and Ca to promote the formation of dolomite and authigenic clays. As far as the Wusongger Formation is concerned, the content of gypsum salt rock is gradually increasing, which may be due to the regression at the end of the Series2 when the carbonate platform was exposed to the surface, resulting in the gradual transition of sedimentary facies from limited platform facies to evaporation platform facies [26,76]. This set of strata encountered during well drilling in the Bachu area is dolomite, gypsum-bearing dolomite mixed with argillaceous dolomite, and upward gypsum salt rock gradually increases and occupies the main position, which indicates that regression occurred during the Wusongger Formation and gradually evolved from limited platform to evaporation lagoon in the Miaolingian [26]. The platform is characterized by significant progradation toward the eastern basin, and the platform and basin are transitioned by gentle slopes [35].

By comparing the research results of the Xiaerblak section with the evolution curve of carbon isotopes of global carbonate rock samples, the global carbon isotopes had significant negative shifts from the end of Series2 to the beginning of Miaolingian (Figure 8). This negative offset and the significant increase in $^{87}\text{Sr}/^{86}\text{Sr}$ are consistent with the mass extinction of Archaeocyathids, Redlichiid, and Olenellid trilobites. The coincidence of these events indicates that they may be caused by the large-scale sea level decline event caused by the enhancement of continental weathering. In the late Series2, the global sea-level decline event [71,72,77] led to the deterioration of the ancient marine environment, such as the exposure of the continental shelf and the shrinking of the marine biosphere, which may have exacerbated the mass extinction.

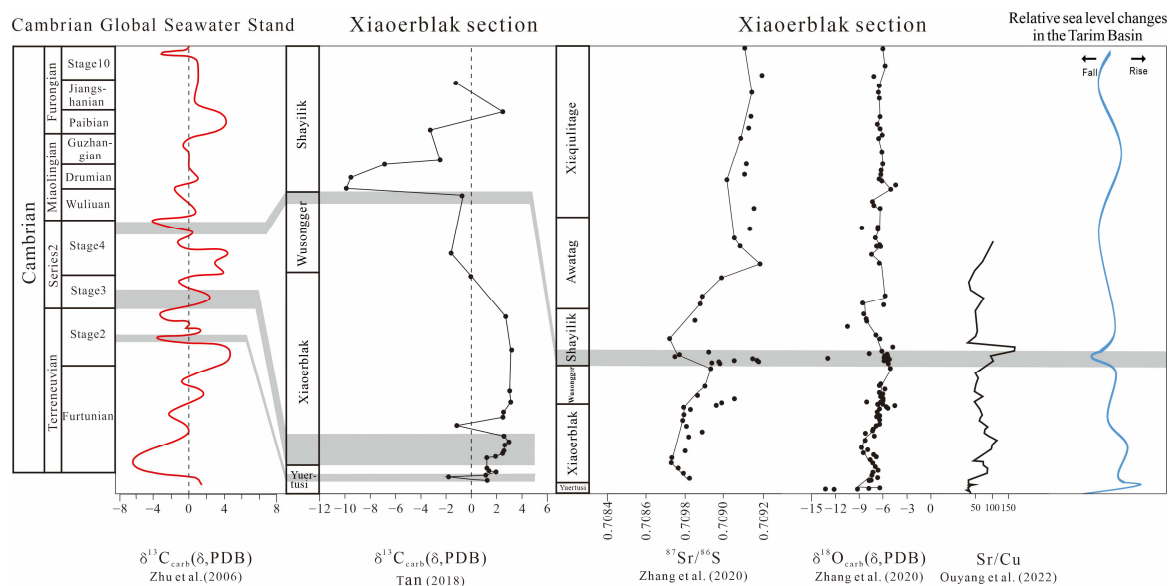


Figure 8. Cambrian global $\delta^{13}\text{C}_{\text{carb}}$ (δ , PDB, peedee belemnite) variation curve [78], the Xiaerblak section $\delta^{13}\text{C}_{\text{carb}}$ (δ , PDB) [77], $^{87}\text{Sr}/^{86}\text{Sr}$, $\delta^{18}\text{O}_{\text{carb}}$ (δ , PDB) [43], and Sr/Cu [32] change curve and corresponding relative sea level change in Tarim Basin.

The sea level gradually rose during the Shayilik Formation, and the water became shallow with the gradual weakening of the transgression during the Shayilik Formation. The sea level fluctuated only slightly during the Awatag period. On the whole, the sea level of the Wusongger–Awatag period is lower than that of the Yuertusi and Xiaerblak periods.

During the Furongian, the relative sea level gradually increased, the water body slowly deepened, the basin was deep in the east and shallow in the west, and the paleogeographic pattern of the third part of the plane was still obvious. The location and distribution of slope facies, open sea shelf facies, and semi-deep sea basin facies changed little. Compared with the Terreneuvian to Miaolingian, the main difference is that the basin ended the evaporation lagoon sedimentary environment and developed a limited platform environment again, which generally reflects the sedimentary background of deeper seawater, slower submarine terrain, and smoother communication between seawater and the outside world [76].

4.4. Oxidation and Reduction Environment

The lower Ce/Ce* (mean value 0.45), higher Y/Ho (mean value 39.77), and higher Eu/Eu* (mean value 35.32), and barite of the Yuertus Formation in the Yutixi section of the Keping area indicate that the ancient ocean in the Keping area was in a seawater environment of reduction and hydrothermal activity at that time [51]. A large number of Ba and Zn elements were enriched. It is believed that the hydrothermal effect can promote the biological eruption and the formation of organic matter by carrying a large number of nutrients. In the early and middle stages, it is an anaerobic oxygen-poor environment ($V/(V + Ni)$ average value is 0.91), with higher total organic carbon (TOC_{max} = 17.2%) and biogenic barium ($ex-Ba = 8634.85 \times 10^{-6}$) showing that the productivity of the ancient ocean is high [31], which proves that the anoxic sedimentary environment is conducive to the preservation of organic matter and is a high-quality hydrocarbon source rock [32,51]. The ancient sea in the early Cambrian Tarim Keping area is an open sea with a rapid water cycle.

From the bottom to the top of the Xiaerblak Formation in the Penglaiba section, redox-sensitive elements showed a consistently increasing trend during transgression, indicating that with the increase in water depth, the transition from an aerobic state to a hypoxic state, and finally to an anoxic stage. Further upward, the opposite trend appeared, and it was an oxygen-rich environment in the Wusongger Formation sedimentation period. This indicates that the seawater is undergoing significant oxidation as it becomes shallower. By comparing the development position of microorganisms in the profile and their corresponding redox conditions, it can be found that the oxygen content of seawater may not be the key factor for the reproduction of microbial flora.

The boundary between the Wusongger Formation and the Shayilik Formation is an obvious $\delta^{13}C$ negative drift, and enrichment of Ba, Ni, V, and other elements, oxidation and reduction indicators such as Th/U, Ni/Co, δCe , δU indicates that the seawater has changed from an oxidizing environment to a reducing environment, indicating that the water body is deepening and reducing, leading to a large number of biological deaths [51]. The red-brown mudstone deposited in the Awatage Formation indicates that it was formed in a strong oxidation sedimentary environment, indicating that the period was in a strong drought and evaporation environment.

5. Conclusions

- (1) The Tarim Basin has gone through the evolution stages of uplift and denudation at the end of the Ediacaran Period, post-rift subsidence, and craton formation in the Early Middle Cambrian, which controlled the transformation of the Tarim Basin from north–south differentiation to the west platform of the east basin, the evolution of gentle slope to the strong rimmed platform, and the distribution and scale of favorable facies in the platform, and developed the muddy rich gentle slope in the sedimentary period of the Yuertus Formation in Terreneuvian, the carbonate gentle slope in the sedimentary period of Series2 Xiaerblak Formation, the weak rimmed platform of the Wusongger Formation in the sedimentary period, and the strong rimmed evaporation platform of Miaolingian and the weak rimmed platform of Furongian.
- (2) Terreneuvian sedimentary framework was mainly controlled by the development of paleo-uplift caused by structure and the change of seawater properties caused

by sea level rise and fall. There is an ancient land not submerged by sea water in Bachu-Tazhong area, which is low in the north and high in the south, laying a basic sedimentary environment. The gentle slope carbonate platform is developed in the Keping area, which is in an open marine environment. The rise and fall of sea levels affect the salinity of seawater from low to high. With the rise of a hydrothermal solution, in an anoxic low oxidation environment, the early sediments are jointly controlled by high paleoproductivity and low oxygen exchange, rich in organic matter, and the salinity is maximum at the end. Dolomites are deposited, thus establishing a shallow water sedimentation model.

- (3) The Series2 widely developed carbonate platform is mainly controlled by sea level rise and fall. From Terreneuvian to Series2, it experienced transgression, and the internal differentiation was controlled by the new paleogeographic pattern of “three uplifts and two depressions”. During the sedimentary period of the Xiaoerbluk Formation and the Wusongger Formation, the Keping area and the Bachu-Tazhong Uplift shifted from deep-water sediments to restricted platform carbonate rocks. During this period, the relative sea level decreased and progradation strengthened. The shallow water begins to develop the dune beach facies belt and platform edge under the high-energy environment. The terrain is gentle and the terrigenous debris is rich. With the hot and dry climate and gradually increasing salinity, it may play an important role in the development of dolomite.
- (4) Under the combined action of rapid accumulation of carbonate rocks, gradual stabilization of global sea level, and the change of paleoclimate from warm and humid to hot and dry, the platform area in the western part of the Tarim Basin changed from a limited platform environment to an evaporation platform environment, and the evaporation lagoon area in Bachu was significantly expanded in the Miaolingian. Under the influence of evaporation, the lithology of the Bachu Uplift belt gradually changed from dark dolomite and red gypsum mudstone to evaporites such as gypsum rock, gypsum salt rock, and salt rock. The Shayilik Formation and the Awatag Formation indicate a strong oxidation environment. The sea level rises, the temperature rises, and the temperature changes from warm and humid to hot and dry. Carbonate rocks in the Bachu–Tazhong area accumulate rapidly, and the water depth becomes shallow, forming evaporation platforms. The lagoon range is significantly expanded, and evaporites such as gypsum rock, gypsum salt rock, and salt rock are developed.
- (5) During the sedimentary period of the Lower Qiulitage subgroup in the Furongian, the climate became warm and humid, the relative sea level gradually increased, and the water depth slowly deepened. The basin ended the evaporation lagoon sedimentary environment and developed a limited platform environment again, which generally reflected the sedimentary background of deeper sea water, slower submarine terrain, and smoother communication between seawater and the outside world.

Author Contributions: X.Y. conceived the idea and K.Z. wrote the initial draft of the paper. Y.W., Y.Z. and J.W. contributed to carrying out additional pictures and editing part of the paper. All authors have read and agreed to the published version of the manuscript.

Funding: This research was funded by National Natural Science Foundation of China (NSFC) (Grants 41972107 and U19B6003), the Fundamental Research Funds for the Central Universities (Grant 2652019078), and the Chinese “111” project (Grant B20011).

Acknowledgments: We thank assistance and/or helpful discussions. We acknowledge anonymous reviewer provided comments that greatly improved the earlier version of this manuscript. We are grateful to our research group members Y.J. Wei, Y.Y. Fang, T.Y. Ma and Y. Lu for their support.

Conflicts of Interest: The authors declare no conflict of interest.

References

1. Zheng, H.R.; Wu, M.B.; Wu, X.W.; Zhang, T.; Liu, C.Y. Oil-gas exploration prospect of dolomite reservoir in the Lower Paleozoic of Tarim Basin. *Acta Pet. Sin.* **2007**, *28*, 1–8. (In Chinese)
2. Huang, H.P.; Zhang, S.C.; Su, J. Palaeozoic oil-source correlation in the Tarim Basin, NW China: A review. *Org. Geochem.* **2016**, *94*, 32–46. [[CrossRef](#)]
3. Cai, C.; Li, K.; Anlai, M.; Zhang, C.; Xu, Z.; Worden, R.H.; Wu, G.; Zhang, B.; Chen, L. Distinguishing Cambrian from Upper Ordovician source rocks: Evidence from sulfur isotopes and biomarkers in the Tarim Basin. *Org. Geochem.* **2009**, *40*, 755–768. [[CrossRef](#)]
4. Chang, X.C.; Wang, T.-G.; Li, Q.M.; Cheng, B.; Tao, X.W. Geochemistry and possible origin of petroleum in Palaeozoic reservoirs from Halahatang Depression. *J. Asian Earth Sci.* **2013**, *74*, 129–141. [[CrossRef](#)]
5. Li, M.; Wang, T.-G.; Shi, S.; Liu, K.; Ellis, G.S. Benzo[b]naphthothiophenes and alkyl dibenzothiophenes: Molecular tracers for oil migration distances. *Mar. Pet. Geol.* **2014**, *57*, 403–417. [[CrossRef](#)]
6. Li, M.; Liu, X.; Wang, T.-G.; Jiang, W.; Fang, R.; Yang, L.; Tang, Y. Fractionation of dibenzofurans during subsurface petroleum migration: Based on molecular dynamics simulation and reservoir geochemistry. *Org. Geochem.* **2018**, *115*, 220–232. [[CrossRef](#)]
7. Cheng, B.; Liao, Z.; Wang, T.; Liu, H.; Tian, Y.; Yang, S. Multiple charges to Sinian reservoirs in the middle Sichuan basin, SW China: Insight from the adsorbed/occluded hydrocarbons in solid bitumens. *J. Pet. Sci. Eng.* **2015**, *127*, 359–366. [[CrossRef](#)]
8. Jin, Z.; Liu, Q.; Yun, J. Potential petroleum sources and exploration directions around the Manjar Sag in the Tarim Basin. *Sci. China Earth Sci.* **2016**, *60*, 235–245. [[CrossRef](#)]
9. Chen, J.; Liu, D.; Hou, X.; Fan, Y.; Jia, W.; Peng, P.; Zhang, B.; Xiao, Z. Origin and evolution of oilfield waters in the Tazhong oilfield, Tarim Basin, China, and their relationship to multiple hydrocarbon charging events. *Mar. Pet. Geol.* **2018**, *98*, 554–568. [[CrossRef](#)]
10. Tang, Y.-J.; Li, M.-J.; Fang, R.-H.; Zhang, B.-S.; Yang, Z.; He, D.-X.; Li, M.-R. Geochemistry and origin of Ordovician oils in the Rewapu Block of the Halahatang Oilfield (NW China). *Pet. Sci.* **2018**, *16*, 1–13. [[CrossRef](#)]
11. Liu, W.; Zhang, G.Y.; Pan, W.Q.; Deng, S.W.; Li, H.H. Lithofacies palaeogeography and sedimentary evolution of the Cambrian in Tarim area. *J. Palaeogeogr.* **2011**, *13*, 529–538. (In Chinese)
12. Qi, L.X. Oil and gas breakthrough in ultra-deep Ordovician carbonate formations in Shuntuoguole uplift, Tarim Basin. *J. China Pet. Explor.* **2016**, *21*, 38–51. (In Chinese)
13. YOU, X.L.; Sun, S.; Zhu, J.Q.; Li, Q.; Hu, W.X.; Dong, H.L. Microbially mediated dolomite in Cambrian stromatolites from the Tarim Basin, north-west China: Implications for the role of organic substrate on dolomite precipitation. *Terra Nova* **2013**, *25*, 387–395. [[CrossRef](#)]
14. YOU, X.L.; Sun, S.; Zhu, J.Q. Significance of fossilized microbes from the Cambrian stromatolites in the Tarim Basin, Northwest China. *Sci. China Earth Sci.* **2014**, *44*, 1777–1790. (In Chinese)
15. YOU, X.L.; Lin, C.S.; Zhu, J.Q.; Tan, J.Y. Primary microbial dolomite precipitation in culture experiments and in stromatolite formations: Implications for the Dolomite Problem. *Carpath. J. Earth Environ.* **2015**, *10*, 197–206.
16. YOU, X.L.; Sun, S.; Lin, C.S.; Zhu, J.Q. Microbial dolomite in the sabkha environment of the middle Cambrian in the Tarim Basin, NW China. *Aust. J. Earth Sci.* **2018**, *65*, 109–120.
17. YOU, X.L.; Jia, W.Q.; Xu, F.; Liu, Y. Mineralogical characteristics of ankerite and mechanisms of primary and secondary origins. *J. Earth Sci. China* **2018**, *43*, 4046–4055.
18. Jia, C.Z.; Pang, X.Q. Research processes and main development directions of deep hydrocarbon geological theories. *Acta Pet. Sin.* **2015**, *36*, 1457–1469.
19. Feng, Z.Z.; Bao, Z.D.; Wu, M.B.; Jin, Z.K.; Shi, X.Z. Lithofacies palaeogeography of the Cambrian in Tarim area. *Front. Earth Sci. China* **2007**, *1*, 265–274. [[CrossRef](#)]
20. Zhao, Z.J.; Luo, J.H.; Zhang, Y.B.; Wu, X.N.; Pan, W.Q. Lithofacies paleogeography of Cambrian sequences in the Tarim Basin. *Acta Pet. Sin.* **2011**, *32*, 937–948.
21. Wu, G.H.; Li, H.W.; Xu, Y.L.; Su, W.; Chen, Z.Y.; Zhang, B.S. The tectonothermal events, architecture and evolution of Tarim craton basement paleo-uplifts. *Acta Petrol. Sin.* **2012**, *28*, 2435–2452.
22. Guan, S.W.; Zhang, C.Y.; Ren, R.; Zhang, Y.C.; Wu, L.; Wang, L.; Ma, P.L.; Han, C.W. Early Cambrian syndepositional structural of the northern Tarim Basin and a discussion of Cambrian subsalt and deep exploration. *Pet. Explor. Dev.* **2019**, *46*, 1075–1086. [[CrossRef](#)]
23. Zhu, Y.J.; Ni, X.F.; Liu, L.L.; Qiao, Z.F.; Chen, Y.Q.; Zheng, J.F. Depositional differentiation and reservoir potential and distribution of ramp systems during post-rift period: An example from the Lower Cambrian Xiaerbulake Formation in the Tarim Basin, NW China. *Acta Sedimentol. Sin.* **2019**, *37*, 1044–1057.
24. Cao, Y.H.; Wang, S.; Zhang, Y.J.; Yang, M.; Yan, L.; Zhao, Y.M.; Zhang, J.L.; Wang, X.D.; Zhou, X.X.; Wang, H.J. Petroleum geological conditions and exploration potential of Lower Paleozoic carbonate rocks in Gucheng Area, Tarim Basin, China. *Pet. Explor. Dev.* **2019**, *46*, 1099–1114. [[CrossRef](#)]
25. Zhang, G.Y.; Liu, W.; Zhang, L.; Yu, B.S.; Li, H.H.; Zhang, B.M.; Wang, L.D. Cambrian-Ordovician prototypic basin, paleogeography and petroleum of Tarim Craton. *Earth Sci. Front.* **2015**, *22*, 269–276.
26. Gao, H.H.; He, D.F.; Tong, X.G.; Wen, Z.X.; Wang, Z.M. Tectonic depositional Environment and Proto-type Basin Evolution of the Cambrian in the Tarim Basin. *Geoscience* **2017**, *31*, 102.

27. Wei, G.Q.; Zhu, Y.J.; Zheng, J.F.; Yu, G.; Ni, X.F.; Yan, L.; Tian, L.; Huang, L.L. Tectonic-lithofacies paleogeography, large-scale source-reservoir distribution and exploration zones of Cambrian subsalt formation, Tarim Basin, NW China. *Pet. Explor. Dev.* **2021**, *48*, 1289–1303.
28. Xiao, Z.H.; Wang, Z.M.; Jiang, R.Q.; Wu, J.C.; Zhang, L.J. Sequence stratigraphic features of the Cambrian carbonate rocks in the Tarim Basin. *Oil Gas Geol.* **2011**, *32*, 1–16.
29. Zheng, J.F.; Zhu, Y.J.; Huang, L.L.; Yang, G.; Hu, F.J. Geochemical Characteristics and Their Geological Significance of Lower Cambrian Xiaerblak Formation in Northwestern Tarim Basin, China. *Minerals* **2022**, *12*, 781.
30. Zheng, J.F.; Pan, W.Q.; Shen, A.J.; Yuan, W.F.; Huang, L.L.; Ni, X.F.; Zhu, Y.J. Reservoir geological modeling and significance of Cambrian Xiaerblak Formation in Keping outcrop area, Tarim Basin, NW China. *Pet. Explor. Dev.* **2020**, *47*, 536–547.
31. Fan, Q.; Fan, T.L.; Li, Y.F.; Zhang, J.P.; Gao, Z.Q.; Chen, Y. Paleo-Environments and Development Pattern of High-Quality Marine Source Rocks of the Early Cambrian, Northern Tarim Platform. *Earth Sci.* **2020**, *45*, 285–302.
32. Ouyang, S.Q.; Lyu, X.X.; Xue, N.; Li, F.; Wang, R. Paleoenvironmental characteristics and source rock development model of the Early-Middle Cambrian: A case of the Keping-Bachu area in the Tarim Basin. *J. China Univ. Min. Technol.* **2022**, *51*, 293–310.
33. Tang, L.J. Major evolutionary stages of Tarim Basin in Phanerozoic Time. *Earth Sci. Front* **1997**, *4*, 318–324.
34. Lin, C.S.; Yang, H.J.; Liu, J.Y.; Peng, L.; Cai, Z.Z.; Yang, X.F.; Yang, Y.H. Paleostuctural geomorphology of the Paleozoic central uplift belt and its constraint on the development of depositional facies in the Tarim Basin. *Sci. China Ser. D Earth Sci.* **2009**, *52*, 823–834. [[CrossRef](#)]
35. Huang, Y.; Fan, T.L.; Berra, F. Architecture and paleogeography of the Early Paleozoic carbonate systems in the east-central Tarim Basin (China): Constraints from seismic and well data. *Mar. Pet. Geol.* **2020**, *113*, 104147.
36. He, B.; Jiao, C.; Xu, Z.; Cai, Z.; Zhang, J.; Li, H.; Chen, W.; Yu, Z. The paleotectonic and paleogeography reconstructions of the Tarim Basin and its adjacent areas (NW China) during the late Early and Middle Paleozoic. *Gondwana Res.* **2016**, *30*, 191–206. [[CrossRef](#)]
37. Ngia, N.R.; Hu, M.Y.; Gao, D. Tectonic and geothermal controls on dolomitization and dolomitizing fluid flows in the Cambrian-Lower Ordovician carbonate successions in the western and central Tarim Basin, NW China. *J. Asian Earth Sci.* **2019**, *172*, 359–382.
38. Gao, Z.Q.; Fan, T.L. Intra-platform tectono-sedimentary response to geodynamic transition along the margin of the Tarim Basin, NW China. *J. Asian Earth Sci.* **2014**, *96*, 178–193.
39. Zhang, J.; Hu, W.; Qian, Y.; Wang, X.; Cao, J.; Zhu, J.; Li, Q.; Xie, X. Formation of saddle dolomites in Upper Cambrian carbonates, western Tarim basin (northwest China): Implications for fault-related fluid flow. *Mar. Pet. Geol.* **2009**, *26*, 1428–1440. [[CrossRef](#)]
40. Jin, Z.; Zhu, D.; Hu, W.; Zhang, X.; Zhang, J.; Song, Y. Mesogenetic dissolution of the middle Ordovician limestone in the Tahe oilfield of Tarim basin, NW China. *Mar. Pet. Geol.* **2009**, *26*, 753–763. [[CrossRef](#)]
41. Wang, K.; Liu, W.; Huang, Q.Y.; Shi, S.Y.; Ma, K.; Liang, D.X. Development characteristics and evolution of the cambrian sedimentary system in Tazhong and gucheng area. Tarim Basin. *Geol. Sci. Technol. Inf.* **2015**, *34*, 116–124. (In Chinese)
42. Liu, W.; Shen, A.J.; Liu, G.D.; Zheng, X.P.; Chen, Y.N.; Zhang, Y. Characteristics and exploration domains of lower paleozoic carbonate reservoirs in eastern Tarim basin. *Mar. Ori. Petrol. Geol.* **2016**, *21*, 1–12. (In Chinese)
43. Zhang, Y.G.; Yang, T.; Hohl, S.V.; Zhu, B.; He, T.C.; Pan, W.Q.; Chen, Y.Q.; Yao, X.Z.; Jiang, S.Y. Seawater carbon and strontium isotope variations through the late Ediacaran to late Cambrian in the Tarim Basin. *Precambrian Res.* **2020**, *345*, 105769. [[CrossRef](#)]
44. Jin, Z.M.; Tan, X.C.; Tang, H.; Shen, A.J.; Qiao, Z.F.; Zheng, J.F.; Li, F.; Zhang, S.X.; Chen, L.; Zhou, C.G. Sedimentary environment and petrological features of organic-rich fine sediments in shallow water overlapping deposits: A case study of Cambrian Yuertus Formation in northwestern Tarim Basin, NW China. *Pet. Explor. Dev.* **2020**, *47*, 513–526. [[CrossRef](#)]
45. Zhou, Z.Y.; Zhao, Z.X.; Hu, Z.X. *Stratigraphy of Tarim Basin*; Science Press: Beijing, China, 2001; pp. 1–359.
46. Zhu, Y.J.; Shen, A.J.; Liu, L.L.; Chen, Y.Q.; Yu, G. Tectonic-sedimentary filling history through the Later Sinian to the Mid-Cambrian in Tarim Basin and its explorational potential. *Acta Sedimentol. Sin.* **2020**, *38*, 398–410.
47. Gao, Z.Q.; Fan, T.L. Carbonate platform-margin architecture and its influence on Cambrian-Ordovician reef-shoal development, Tarim Basin, NW China. *Mar. Pet. Geol.* **2015**, *68*, 291–306. [[CrossRef](#)]
48. Zhang, Z.Y.; Zhu, G.Y.; Zhang, Y.J.; Han, J.F.; Li, T.T.; Wang, E.; Greenwood, P. The origin and accumulation of multi-phase reservoirs in the east Tabei uplift, Tarim Basin, China. *Mar. Pet. Geol.* **2018**, *98*, 533–553. [[CrossRef](#)]
49. Jiang, W.; Gao, Z.Q.; Hu, Z.Q.; Chu, C.L. Sedimentary Filling Evolution and Hydrocarbon Control of High Frequency Sequence in Yurtus Formation, Tarim Basin. *Geoscience* **2021**, *35*, 349–364.
50. Xie, L. Study of Marine Carbonate Source Rocks in the Lower Paleozoic: The Lower Cambrian Xiaerbulake Formation in Tarim basin. Master's Thesis, China University of Petroleum, Beijing, China, 2016.
51. Fan, Q.Q.; Lu, S.F.; Li, W.H.; Pan, W.Q.; Zhang, B.S.; Zhang, Y.Y.; Tan, Z.Z. Geochemical characteristics and geological significance for petroleum of the Middle-Lower Cambrian marine strata: A case study of Keping area in the Tarim basin. *J. China Univ. Min. Technol.* **2019**, *48*, 377–394.
52. Ren, Y.G.; Zhang, J.L.; Qi, J.S.; Zhang, Y.J.; Zhang, B.; Liu, Y. Sedimentary characteristics and evolution laws of cambrian-ordovician carbonate rocks in Tadong region. *Pet. Geol. Oilfield Dev. Daqing* **2014**, *33*, 103–110. (In Chinese)
53. Wang, G.; Fan, T.L.; Liu, H.H. Characteristics and evolution of ordovician carbonate platform marginal facies in tazhong-gucheng area. Tarim Basin. *Geoscience* **2014**, *28*, 995–1007. (In Chinese)

54. Xu, X.S.; Wang, Z.J.; Wan, F.; Fu, H. Tectonic paleogeographic evolution and source rocks of the early paleozoic in the Tarim Basin. *Earth Sci. Front.* **2005**, *12*, 49–57. (In Chinese)
55. Lin, C.S.; Li, S.T.; Liu, J.Y.; Qian, Y.X.; Luo, H.; Chen, J.Q.; Peng, L.; Rui, Z.F. Tectonic framework and paleogeographic evolution of the Tarim basin during the Paleozoic major evolutionary stages. *Acta Petrol. Sin.* **2011**, *27*, 210–218. (In Chinese)
56. Wang, Q.; Li, S.Z.; Zhao, S.J.; Mu, D.L.; Guo, R.H.; Somerville, I. Early paleozoic Tarim Orocline: Insights from paleogeography and tectonic evolution in the Tarim. *Basin Geol. J.* **2017**, *52*, 436–448. [[CrossRef](#)]
57. Li, S.; Yang, Z.; Zhao, S.; Li, X.; Guo, L.; Yu, S.; Liu, X.; Suo, Y.; Lan, H. Global Early Paleozoic orogens (I): Collision-type orogeny. *J. Jilin Univ. Earth Sci. Ed.* **2016**, *46*, 945–967. (In Chinese)
58. Li, S.; Zhao, S.; Liu, X.; Cao, H.; Yu, S.; Li, X.; Somerville, I.; Yu, S.; Suo, Y. Closure of the Proto-Tethys Ocean and Early Paleozoic amalgamation of microcontinental blocks in East Asia. *Earth-Sci. Rev.* **2018**, *186*, 37–75. [[CrossRef](#)]
59. Jia, C.Z.; Zhang, S.B.; Wu, S.Z. *Stratigraphy of the Tarim Basin and Adjacent Areas*; Science Press: Beijing, China, 2004; pp. 1–450.
60. He, D.F. Cenozoic tectonic evolution and oil-gas accumulation in Tarim basin. *Pet. Explor. Dev.* **1994**, *21*, 1–8.
61. He, D.F.; Jia, C.Z.; Li, D.S.; Zhang, C.J.; Meng, Q.R.; Shi, X. Formation and evolution of polycyclic superimposed Tarim Basin. *Oil Gas Geol.* **2005**, *26*, 64–77.
62. Feng, Z.Z.; Peng, Y.M.; Jin, Z.L.; Bao, Z.D. Lithofacies palaeogeography of the early Cambrian in China. *J. Palaeogeogr.* **2002**, *4*, 1–12.
63. Liu, P.X.; Guan, P.; Feng, F.; Jia, W.B.; Zhang, W.; Deng, S.B.; Jin, Y.Q. Evolution of Cambrian Sedimentary Environment and Ocean-Land Coupling of the Western Tarim Carbonate Platform. *Acta Sedimentol. Sin.* **2016**, *34*, 1092–1107.
64. Lan, X.D.; Lü, X.X.; Zhu, Y.M.; Yu, H.F. The geometry and origin of strike-slip faults cutting the Tazhong low rise megaanticline (central uplift, Tarim Basin, China) and their control on hydrocarbon distribution in carbonate reservoirs. *J. Nat. Gas Sci. Eng.* **2015**, *22*, 633–645. [[CrossRef](#)]
65. Li, S.; Yang, Z.; Zhao, S.; Li, X.; Suo, Y.; Guo, L.; Yu, S.; Dai, L.; Li, S.; Mu, D. Global Early Paleozoic orogens (II): Subduction-accretionary-type orogeny. *J. Jilin Univ. Earth Sci. Ed.* **2016**, *46*, 968–1004. (In Chinese)
66. Li, S.; Yang, Z.; Yang, Z.; Zhao, S.; Liu, X.; Yu, S.; Li, X.; Guo, L.; Suo, Y.; Dai, L.; et al. Global Early Paleozoic (IV): Plate reconstruction and supercontinent Carolina. *J. Jilin Univ. Earth Sci. Ed.* **2016**, *46*, 1026–1041. (In Chinese)
67. Li, S.; Zhao, S.; Li, X.; Cao, H.-H.; Liu, X.; Guo, X.; Xiao, W.; Lai, S.; Yan, Z.; Li, Z.; et al. Tethys Ocean in East Asian (I): Northern and southern border faults and subduction polarity. *Acta Petrol. Sin.* **2016**, *32*, 2609–2627. (In Chinese)
68. Li, S.Z.; Zhao, S.J.; Yu, S.; Cao, H.H.; Li, X.Y.; Liu, X.; Guo, X.; Xiao, W.; Lai, S.; Yan, Z.; et al. Proto-Tethys Ocean in east Asian (II): Affinity and assembly of Early Paleozoic micro-continental blocks. *Acta Petrol. Sin.* **2016**, *32*, 2628–2644. (In Chinese)
69. Liu, H.; Somerville, I.D.; Lin, C.S.; Zuo, S.J. Distribution of Palaeozoic tectonic superimposed unconformities in the Tarim Basin, NW China: Significance for the evolution of palaeogeomorphology and sedimentary response. *Geol. J.* **2016**, *51*, 627–651.
70. Shao, L.Y.; Dou, J.W.; Zhang, P.F. Paleogeographic Significances of Carbon and Oxygen Isotopes in late Permian Rocks of Southwest China. *Geochimica* **1998**, *06*, 575–581.
71. Mei, M.X.; Ma, Y.S.; Zhang, H.; Meng, X.Q.; Chen, Y.H. From Basin Black Shales to Platform Carbonate Rocks: A Study on Sequence Stratigraphy for the Lower Cambrian of the Upper-Yangtze Region in South China. *Acta Geol. Sin. Engl. Ed.* **2007**, *81*, 739–755.
72. Zuo, J.X.; Peng, S.C.; Qi, Y.P.; Zhu, X.J.; Bagnoli, G.; Fang, H.B. Carbon-Isotope Excursions Recorded in the Cambrian System, South China: Implications for Mass Extinctions and Sea-Level Fluctuations. *J. Earth Sci.* **2018**, *29*, 479–491.
73. Song, Y.F.; Chen, D.Z.; Guo, C.; Zhou, X.Q. Depositional Characteristics of Microbial Carbonates from the Lower Xiaerbulak Formation in the Xiaerbulake Section, Tarim Basin. *Acta Sedimentol. Sin.* **2020**, *38*, 55–63.
74. Fang, Y.H.; Xu, H.F. Dissolved silica-catalyzed disordered dolomite precipitation. *Am. Mineral.* **2022**, *107*, 443–452. [[CrossRef](#)]
75. Fang, Y.H.; Xu, H.F. Coupled dolomite and silica precipitation from continental weathering during deglaciation of the Marinoan Snowball Earth. *Precambrian Res.* **2022**, *380*, 106824. [[CrossRef](#)]
76. Jing, S. Lithic Facies and Geochemical Characteristics of Cambrian Dolomite in the Bachu Uplift Belt, Tarim Basin. Master's Thesis, Xi'an Shiyou University, Xi'an, China, 2020.
77. Tan, Z.Z. Depositional environment and controlling factors of Cambrian-Ordovician marine carbonate in the Tarim Basin. Master's Thesis, China University of Petroleum (East China), Qingdao, China, 2018.
78. Zhu, M.Y.; Babcock, L.E.; Peng, S.C. Advances in Cambrian stratigraphy and paleontology: Integrating correlation techniques, paleobiology, taphonomy and paleoenvironmental reconstruction. *Palaeoworld* **2006**, *15*, 217–222.

Disclaimer/Publisher's Note: The statements, opinions and data contained in all publications are solely those of the individual author(s) and contributor(s) and not of MDPI and/or the editor(s). MDPI and/or the editor(s) disclaim responsibility for any injury to people or property resulting from any ideas, methods, instructions or products referred to in the content.